

Human Mesenchymal Stem Cell Secretome Exhibits a Neuroprotective Effect over *In Vitro* Retinal Photoreceptor Degeneration

Ricardo Usategui-Martín,¹ Kevin Puertas-Neyra,¹ María-Teresa García-Gutiérrez,¹ Manuel Fuentes,^{2,3} José Carlos Pastor,^{1,4,5,6} and Ivan Fernandez-Bueno^{1,5,6}

¹Instituto Universitario de Oftalmobiología Aplicada (IOBA), Retina Group, Universidad de Valladolid, 47011 Valladolid, Spain; ²Proteomics Unit, Cancer Research Centre (IBMCC/CSIC), University of Salamanca, Institute of Biomedical Research of Salamanca (IBSAL), 37007 Salamanca, Spain; ³Department of Medicine and General Cytometry Service-Nucleus, CIBERONC CB16/12/00400, Cancer Research Centre (IBMCC/CSIC), University of Salamanca, Institute of Biomedical Research of Salamanca (IBSAL), 37007 Salamanca, Spain; ⁴Department of Ophthalmology, Hospital Clínico Universitario de Valladolid, 47003 Valladolid, Spain; ⁵Centro en Red de Medicina Regenerativa y Terapia Celular de Castilla y León, 47011 Valladolid, Spain; ⁶Red Temática de Investigación Cooperativa en Salud (RETICS), Oftared, Instituto de Salud Carlos III, 47011 Valladolid, Spain

Retinal photoreceptor degeneration occurs frequently in several neurodegenerative retinal diseases such as age-related macular degeneration, retinitis pigmentosa, or genetic retinal diseases related to the photoreceptors. Despite the impact on daily life and the social and economic consequences, there is no cure for these diseases. Considering this, cell-based therapy may be an optimal therapeutic option. This study evaluated the neuroprotective *in vitro* potential of a secretome of human bone marrow mesenchymal stem cells (MSCs) for retinal photoreceptors *in vitro*. We analyzed the photoreceptor morphologic changes and the paracrine factors secreted by human bone marrow MSCs in a physically separated co-culture with degenerated neuroretinas, using organotypic neuroretinal cultures. The results showed that the secretome of human bone marrow MSCs had a neuroprotective effect over the neuroretinal general organization and neuropreserved the photoreceptors from degeneration probably by secretion of neuroprotective proteins. The study of the expression of 1,000 proteins showed increased paracrine factors secreted by MSCs that could be crucial in the neuroprotective effect of the stem cell secretome over *in vitro* retinal degeneration. The current results reinforce the hypothesis that the paracrine effect of the human bone marrow MSCs may slow photoreceptor neurodegeneration and be a therapeutic option in retinal photoreceptor degenerative diseases.

INTRODUCTION

Retinal neurodegeneration, the main pathogenic mechanism involved in multiple eye diseases that are the most frequent causes of incurable low vision and blindness worldwide, includes retinal deterioration resulting from different causes that leads to progressive degeneration and cellular death. This neuronal death usually is accompanied by a glial cell response that replaces the visual neurons. Retinal photoreceptor degeneration occurs frequently in several neurodegenerative

retinal diseases, e.g., age-related macular degeneration, diabetic retinopathies, retinitis pigmentosa, and genetic retinal diseases related to the photoreceptors.¹ Reportedly, 240 million patients have photoreceptor-related degeneration worldwide.²

Despite the impact on daily life and the social and economic consequences, there is no cure for most retinal diseases in which photoreceptor atrophy and death are the main causes of impaired vision. Advanced therapies may be treatment options, of which cell-based therapy may be one of the most viable alternatives. Current research in stem cell therapy for retinal neurodegeneration is based on two main therapeutic approaches: replacement of damaged cells and neuroprotection via the paracrine stem cell properties.^{1,3,4} Cell-based therapy via the paracrine neuroprotective effects may be the most promising alternative. Although it has been reported that stem cell-derived photoreceptors may integrate and/or transfer material to the retinal cells,^{5–7} other studies have suggested that the retina does not provide a permissive environment in which stem cells can migrate, integrate, and function.^{6,8,9} However, several proteins secreted by stem cells are associated with a slowdown of the retina neurodegenerative process.^{1,10,11} Thus, advanced investigations to determine the composition of the stem cell neuroprotective secretome are crucial and will be the basis for future production of cell-free “secretome cocktails” with effective neuroprotective capacity over retinal degenerative diseases.

The cells that are studied most in cell-based therapy are mesenchymal stem cells (MSCs) because they are rapidly expandable, easily isolated,

Received 30 April 2020; accepted 7 May 2020;
<https://doi.org/10.1016/j.omtm.2020.05.003>.

Correspondence: Ivan Fernandez-Bueno, DVM, PhD, Instituto Universitario de Oftalmobiología Aplicada (IOBA), Retina Group, Universidad de Valladolid, Campus Miguel Delibes, Paseo de Belén 17, 47011 Valladolid, Spain.

E-mail: ifernandezb@ioba.med.uva.es



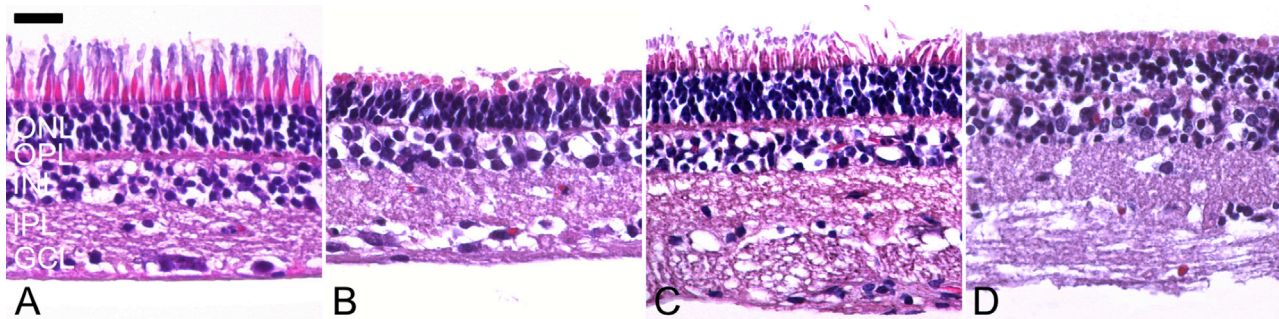


Figure 1. General Morphology of Neuroretinas

(A–D) Neuroretinas general morphology before *in vitro* culture (A), after 3 days of culture (B), after co-culture with mesenchymal stem cells from Valladolid (MSCVs) for 3 days (C), and after co-culture with HEK293T cells for 3 days (D). Scale bar, 25 μm .

and are not associated with ethical issues.^{12,13} MSCs also are hypoinmunogenic or immunoprivileged because the major histocompatibility complex of class II (MHC-II) or the co-stimulatory molecules (CD40, CD80, and CD86) involved in transplant rejection are not expressed on their surface.¹⁴ However, some studies have suggested that cell-mediated and humoral immune responses to MHC mismatched with MSCs occur and the authors thereby defined the MSCs as immune evasive.^{15,16} Therefore, allogeneic transplantation of these cells has attractive advantages because they do not require host immunosuppression.¹⁴

In our previous studies, we have reported that the intravitreal injection of human MSCs is safe, well tolerated, and bio-available in the vitreous cavity from 2 to 6 weeks.¹⁷ This study was requested by the Spanish Agency for Drugs and Medical Devices before the authorization to use MSCs in a phase I/II clinical trial to evaluate the safety of intravitreal injection of human MSCs in patients with non-arteritic acute ischemic optic neuropathy (ClinicalTrials.gov: NCT03173638). Also, we have established that human MSCs improve the survival and maintenance of retinal ganglion cells (RGCs) via the paracrine neuroprotective potential of the MSCs.¹¹ Our hypothesis is based on the idea that the paracrine effect of the human bone marrow MSCs also may produce a slow photoreceptor neurodegeneration. Thus, the current study evaluated *in vitro* the potential neuroprotection effect of human bone marrow MSCs in a porcine retinal photoreceptor degeneration model and identified some of the paracrine factors secreted in co-cultures of neuroretinas with human stem cells.

RESULTS

Neuroretinal General Morphology, Morphometry, and Nuclei Counts

The results of the analyses of the neuroretinal general morphology, morphometry, and nuclei counts are summarized in Figures 1 and 2. Fresh porcine neuroretinal samples had a clearly defined layered retinal structure and adequate cellular preservation before culturing, with perfectly defined photoreceptor outer segments (OSs) and inner segments (ISs) (Figure 1A). The mean total neuroretinal thickness was $177.24 \pm 1.65 \mu\text{m}$ (Figure 2A) and the mean number of nuclei/ μm^2 was 124.33 ± 1.53 (Figure 2B).

The general layered structure of the neuroretinas was preserved after 72 h of culture but with extensive photoreceptor degeneration. The OS photoreceptors were primarily absent, and those in the ISs were shortened, compacted, and edematous (Figure 1B) compared with the fresh controls. The thicknesses of the outer nuclear layer (ONL), outer plexiform layer (OPL), inner nuclear layer (INL), and ganglion cell layer (GCL) were decreased significantly compared with the fresh neuroretinas (Figure 2A). The mean total number of nuclei/ μm^2 (88.66 ± 4.04) and the number of nuclei/ μm^2 in the ONL were also lower than in the fresh neuroretina (Figure 2B).

The neuroretinas co-cultured with MSCs from Valladolid (MSCVs) for 72 h were better preserved with shortened rod OSs and edematous cone ISs (Figure 1C). Compared with the fresh neuroretinas, there were no significant differences in the total thickness ($183.06 \pm 10.89 \mu\text{m}$) and the retinal layer thickness (Figure 2A) or in the total number of nuclei/ μm^2 (125 ± 1) and the number of nuclei/ μm^2 /layer (Figure 2B).

In the neuroretinas co-cultured with HEK293T cells for 72 h, the degenerative neuroretinal modifications were similar to those observed in the neuroretinas after 72 h in the untreated retinal culture. The OS and IS photoreceptors were not differentiated and nuclear layer disorganization was observed (Figure 1C). The ONL, OPL, INL, and GCL were significantly thinner than the fresh neuroretinas and the neuroretinas co-cultured with MSCVs for 72 h (Figure 2A). There were fewer total numbers of nuclei/ μm^2 (88.66 ± 4.04) and nuclei/ μm^2 in the ONL compared with the fresh neuroretinas and the neuroretinas co-cultured with MSCVs for 72 h (Figure 2B).

Immunochemical Characterization

The peanut agglutinin (PNA) lectin marker was used to identify and evaluate the cones (Figures 3A–3D). PNA is specific for galactosyl-(β -1,3)-*N*-acetylgalactosamine; therefore, PNA lectin binds to the extracellular matrix around the cone OSs.²² The immunoexpression of PNA lectin in fresh neuroretinas was uniformly distributed in the cone OSs (Figure 3A). After 72 h of culture, the neuroretinas showed minute expression of PNA lectin with a heterogeneous

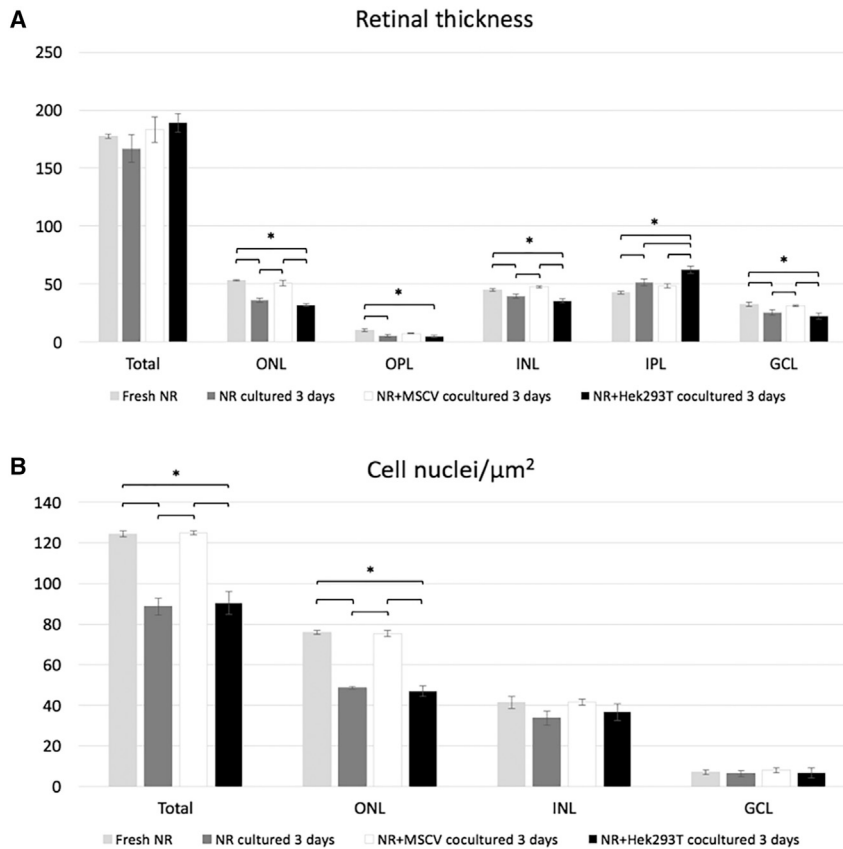


Figure 2. Neuroretinal Morphometry

(A and B) Comparison of neuroretinal morphometry (A) and nuclei counts (B) in fresh neuroretinas, neuroretinas cultured for 3 days, neuroretinas co-cultured with MSCVs for 3 days, and neuroretinas co-cultured with HEK293T cells for 3 days. NR, neuroretina. * $p < 0.05$.

shortened rods in the neuroretina OSs co-cultured with MSCVs (Figure 3G). There were no significant ($p = 0.697$) differences in the Rho protein immunorexpression between fresh neuroretinas and neuroretinas co-cultured with MSCVs (Figure 4B). The Rho protein immunorexpression in the neuroretinas co-cultured with HEK293T cells was similar to the neuroretinas cultured for 72 h (Figure 3H). The results showed significantly ($p < 0.001$ for both comparisons) higher Rho protein immunorexpression when the neuroretinas co-cultured with MSCVs and neuroretinas after 72 h of culture were compared and when neuroretinas co-cultured with MSCVs and neuroretinas co-cultured with HEK293T cells were compared (Figure 4B).

To analyze the morphology of the rod bipolar cells, the immunorexpression of protein kinase α (PKC α) protein was determined (Figures 3I–3L). PKC α modulates rod bipolar cell function by accelerating the glutamate-driven signal transduction and termination.¹⁹ The PKC α immunorexpression in the fresh neuroretinas was uniformly distributed along with the cytoplasm of the bipolar cells through the INL and inner plexiform layer (IPL), and the immunofluorescence was more intense in their terminal buttons (Figure 3I). Reduced PKC α protein immunorexpression with heterogeneous distribution in the rod bipolar cells (Figure 3J) was seen in the neuroretinas mono-cultured for 72 h; in the neuroretinas co-cultured with MSCVs for 72 h, the PKC α protein showed similar immunorexpression to that in fresh neuroretinas but with reduced fluorescence intensity at their terminal buttons (Figure 3K). No significant ($p = 0.762$) differences were seen in the PKC α protein immunorexpression between the fresh neuroretinas and neuroretinas co-cultured with MSCVs (Figure 4C). In the neuroretinas co-cultured with the HEK293T cells, the PKC α immunorexpression was close to that of the neuroretinas cultured for 72 h (Figure 3L). The results showed significantly ($p = 0.003$ and $p = 0.002$, respectively) and higher PKC α protein immunorexpression between the neuroretinas co-cultured with MSCVs and neuroretinas after 72 h of culture and between the neuroretinas co-cultured with MSCVs and neuroretinas co-cultured with HEK293T cells (Figure 4C).

To analyze the gliosis and retinal degeneration, the immunorexpression of glial fibrillary acidic protein (GFAP) was studied (Figures 3M–3P). Gliosis is an indicator of glial cell activation that is analyzed

distribution in the remaining compacted OSs (Figure 3B). The neuroretinas co-cultured with MSCVs showed shortened cone OSs expressing PNA and slight displacement around the IS region (Figure 3C). There were no significant ($p = 0.872$) differences in the PNA lectin immunorexpression between the fresh neuroretinas and those co-cultured with MSCVs (Figure 4A). Regarding the neuroretinas co-cultured with HEK293T cells, the PNA lectin immunorexpression was similar to the neuroretinas cultured for 72 h corresponding to degenerated cones (Figure 3D). The results showed significantly ($p < 0.001$ for both comparisons) higher PNA lectin immunorexpression when the neuroretinas co-cultured with MSCVs and neuroretinas cultured for 72 h were compared and when the neuroretinas co-cultured with MSCVs and those co-cultured with HEK293T cells were compared (Figure 4A). To identify and analyze the rods, we studied the immunorexpression of rhodopsin (Rho) protein (Figures 3E–3H). Rho is synthesized in the rough endoplasmic reticulum, packaged in the Golgi apparatus, transported through the IS cytoplasm to the connecting cilium, and inserted into newly forming membrane discs at the base of the OSs; therefore, Rho immunorexpression is located in the rod outer discs.¹⁸ The immunorexpression of Rho protein in fresh neuroretinas was distributed homogeneously in the rod OSs (Figure 3E). Almost no Rho protein immunorexpression was seen in the neuroretinas cultured for 72 h, and the distribution was limited to the remaining degenerated rods (Figure 3F). The results showed maintenance of the Rho immunorexpression in the

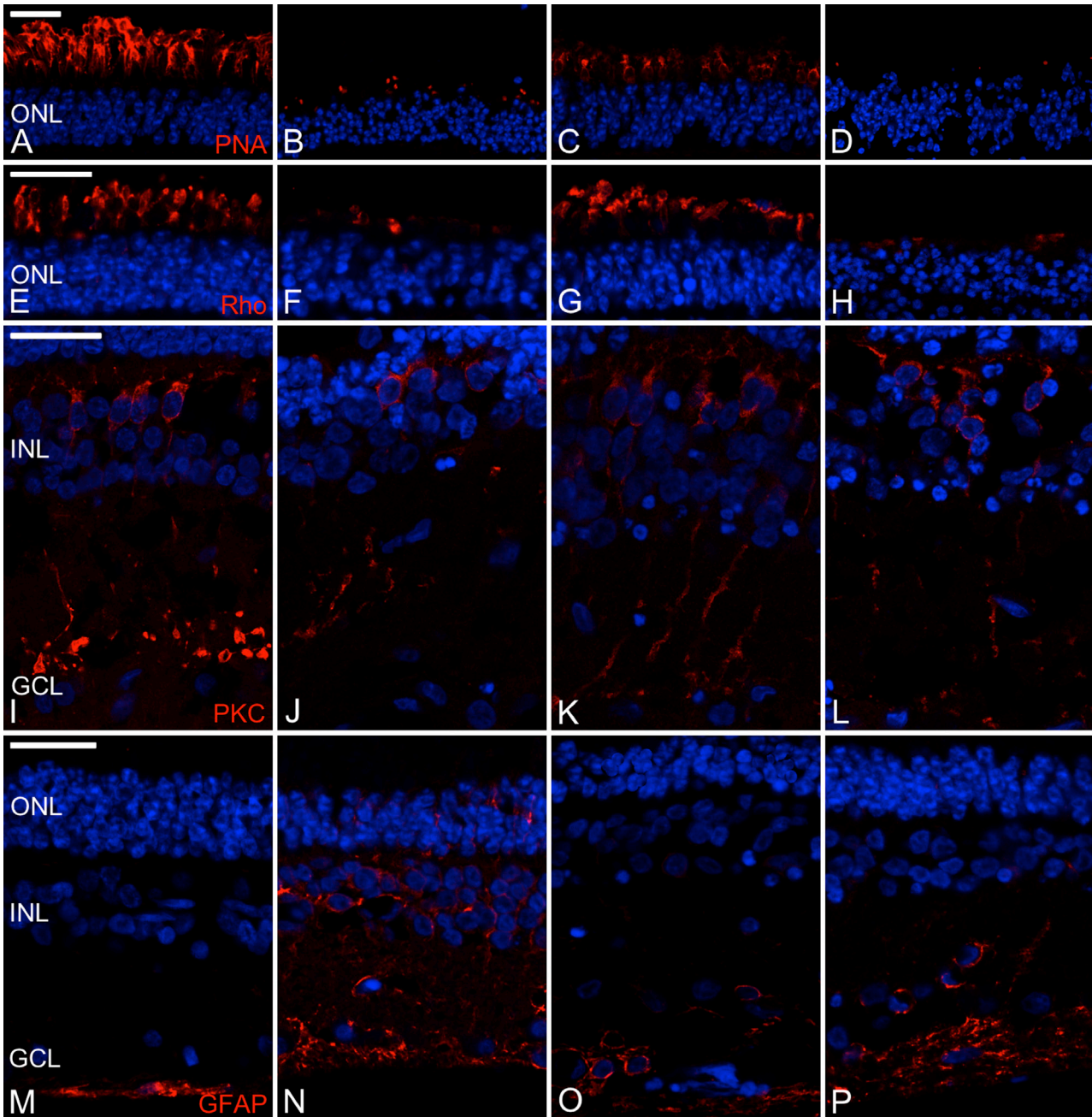


Figure 3. Immunofluorescence Characterization

(A–D) Immunofluorescence expression of the peanut agglutinin (PNA) lectin protein in fresh neuroretinas (A), neuroretinas cultured for 3 days (B), neuroretinas co-cultured with MSCVs for 3 days (C), and neuroretinas co-cultured with HEK293T cells for 3 days (D). (E–H) Immunofluorescence expression of the rhodopsin (Rho) protein in fresh neuroretinas (E), neuroretinas cultured for 3 days (F), neuroretinas co-cultured with MSCVs for 3 days (G), and neuroretinas co-cultured with HEK293T cells for 3 days (H). (I–L) Immunofluorescence expression of protein kinase C α (PKC α) in fresh neuroretinas (I), neuroretinas cultured for 3 days (J), neuroretinas co-cultured with MSCVs for 3 days (K), and neuroretinas co-cultured with HEK293T cells for 3 days (L). (M–P) Immunofluorescence expression of the glial fibrillary acidic protein (GFAP) in fresh neuroretinas (M), neuroretinas cultured for 3 days (N), neuroretinas co-cultured with MSCVs for 3 days (O), and neuroretinas co-cultured with HEK293T cells for 3 days (P). Scale bars, 25 μ m.

by GFAP immunoreaction. GFAP is expressed in glial cells in response to retinal degeneration.²⁰ In the fresh neuroretinas, the GFAP immunofluorescence was restricted to the retinal ganglion layer

(RGL) and nerve fiber layer (NFL) (Figure 3M). The GFAP immunofluorescence in the mono-cultured neuroretinas showed invasion of the cytoplasm of the glial cells to the INL and even the ONL

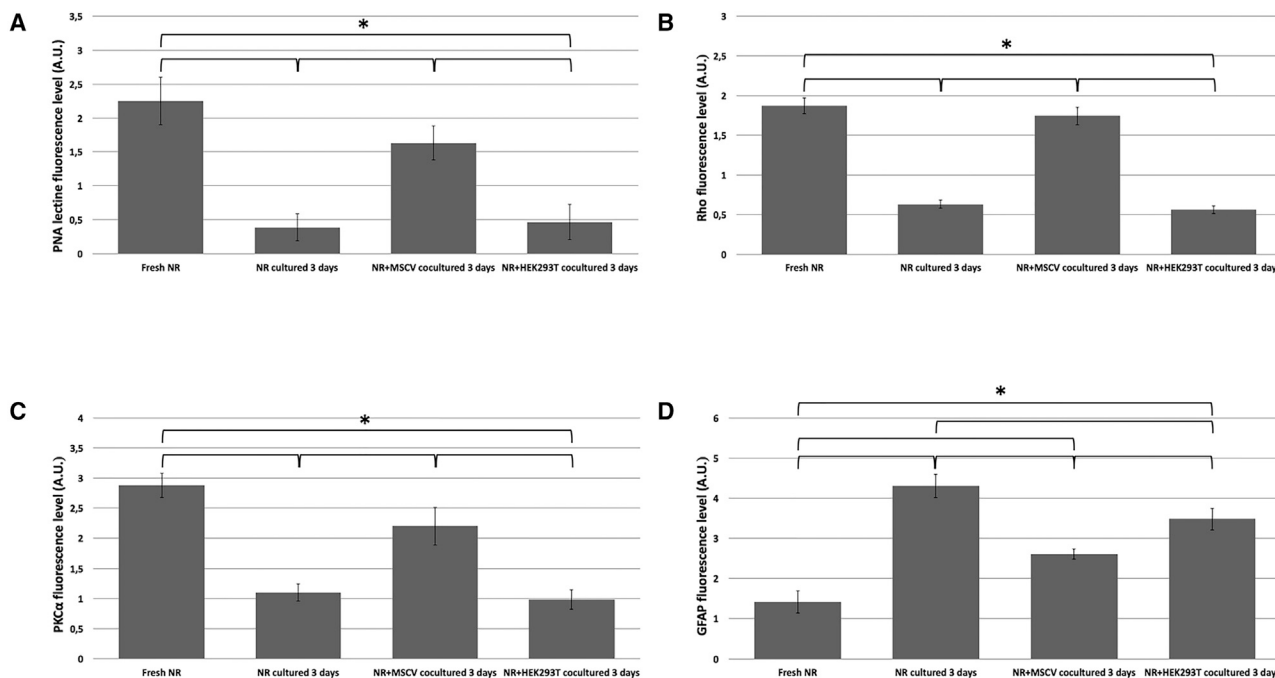


Figure 4. Semiquantitative Immunohistochemical Analysis

(A–D) Immunoexpression of the PNA lectin protein (A), Rho protein (B), PKC α (C), and GFAP (D). * $p < 0.05$. A.U., arbitrary units; NR, neuroretina.

(Figure 3N). GFAP immunoexpression distributed throughout the RGL and in the IPL (Figure 3O) was seen in neuroretinas co-cultured with MSCVs. In the neuroretinas co-cultured with HEK293T cells, the immunoexpression of GFAP extended to the outermost INL regions without reaching the ONL (Figure 3P). All of the comparisons reached significance (Figure 4D).

MSC Surface Marker Evaluation

MSC viability was greater than 95% in all experimental conditions. MSC cultures were confluent before co-culturing with the porcine neuroretinal explants. The results of the surface marker evaluation showed that mono-cultured and co-cultured MSCVs were positive for CD44, CD90, STRO1, and CD146 and negative for the CD14 and CD16 cell surface markers (Figure 5).

Analysis of the Protein Profile

To identify possible paracrine factors secreted by MSCVs that may be implicated in slowing retinal neurodegeneration, the differential profiles of secreted proteins by MSCVs in the presence and absence of retinas in neurodegeneration were analyzed. The results showed statistically significant differences in the relative protein abundance profile of 653 proteins, of which 152 proteins were higher in the mono-cultured MSCVs than in the MSCVs co-cultured with neuroretinas, and 501 proteins were higher in MSCVs co-cultured with neuroretinas than those cultured alone (Table 1; Table S1). These proteins were involved in inflammation, immunity, death, cellular survival, stress, cellular oxidation, collagen metabolism, lipid metabolism, calcium metabolism, retinol metabolism, and angiogenesis

processes. Table 2 summarizes the more relevant proteins with expression levels that were significantly higher in the MSCVs co-cultured with neuroretinas than in the mono-cultured MSCVs.

DISCUSSION

Many neurodegenerative retinal diseases are characterized by photoreceptor degeneration.¹ Despite the impact on daily life and social and economic consequences, there is no cure for these diseases, and cell therapy based on the paracrine properties of stem cells may be a therapeutic option.^{1,3,4} Our previous experiments showed the biocompatibility of intravitreal injection of human MSCs and that they can improve the survival and maintenance of RGCs through paracrine neuroprotective potential.^{11,17} We hypothesized that the paracrine effect of the human bone marrow stem cells may slow photoreceptor neurodegeneration. Therefore, the current study evaluated *in vitro* the neuroprotective potential of the MSC secretome over retinal photoreceptors using an *ex vivo* model of spontaneous neuroretinal degeneration. This is the first study analyzing the MSC secretome under experimental neuroretina degeneration, as this condition seems crucial since the extracellular environment would influence the secretome composition and, thus, induce its neuroprotective effect.

Organ retinal explant cultures are useful for studying neurodegeneration and neuroprotection processes because they bridge the gap between cell cultures and animal models. Organ retinal explant cultures also replicate, with *in vitro* limitations, the cellular changes that occur in the retina *in vivo*. The principal limitations of organ retinal explant cultures are the axotomy of the RGCs and the absence of a blood

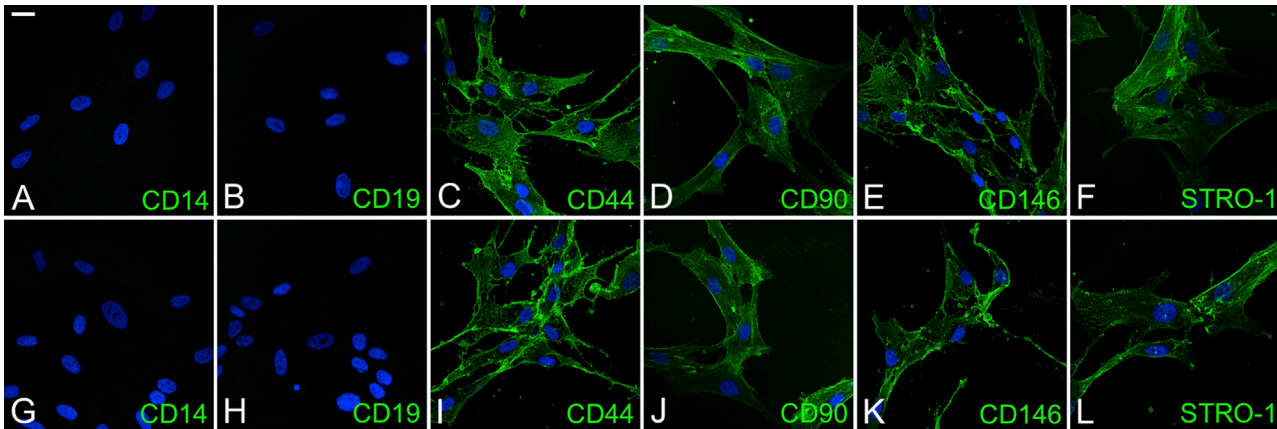


Figure 5. Mesenchymal Stem Cell (MSC) Surface Marker Evaluation

(A–L) MSC surface markers after 3 days of culture (A, CD14; B, CD19; C, CD44; D, CD90; E, CD146; F, STRO-1) and after co-culture with neuroretina explants for 3 days (G, CD14; H, CD19; I, CD44; J, CD90; K, CD146; L, STRO-1). Scale bar, 25 μ m.

supply and retinal pigment epithelium. Despite these limitations, organ retinal explant cultures are an excellent resource to study retinal neurodegeneration.^{21,23} In the current study, neuroretinal explants were cultured over porous cell culture membranes that prevented the cells from migrating and integrating into the retinal tissue. We performed the study using stem cells and non-stem cells (HEK293T cells) as a negative control of neuroprotection with the objective to demonstrate that only stem cells (through their paracrine properties) show a neuroprotective effect over degenerating neuroretina.

Neuroretinas co-cultured with MSCVs for 72 h had better preserved structural organization than did mono-cultured neuroretinas. The glial response showed that GFAP expression was lower in neuroretinas co-cultured with MSCVs than in mono-cultured neuroretinas. GFAP is expressed in the astrocytes and Müller cells and is associated with glial activation as a consequence of the neurodegenerative process.^{20,24} Our findings suggested that MSCV paracrine properties have a neuroprotective effect in neuroretina against degeneration, results that are in complete agreement with previous reports.^{11,25,26} Those studies focused on the evaluation of RGCs or the neuroprotective properties of the human neural progenitor cells (hNPCs); therefore, to the best of our knowledge, this is the first study to evaluate the neuroprotective potential of human bone marrow MSCs over the retinal photoreceptor layer. Our results showed that the immunoprotein levels of PNA lectin, Rho, and PKC α proteins were similar in the neuroretinas co-cultured with MSCVs for 72 h and in the fresh neuroretinas, which may have resulted from the MSCV neuroprotective effect over cones, rods, and rod bipolar cells. These results agreed with those reported previously in organ retinal explant cultures, which determined that hNPCs slow the spontaneous photoreceptor degenerative process.^{25,26} hNPCs are a type of embryonic stem cell associated with ethical and political controversies. Human MSCs could be the best option for cell therapy strategies because their use does not present ethical problems and they are immunoprivileged¹⁴ or immune evasive.^{15,16} Thus, allogeneic transplantation of human

bone marrow MSCs has the critical advantage of not requiring host immunosuppression,¹⁴ and retinal neuroprotection via MSC paracrine effects is currently viable.^{11,12}

Stem cell therapy for retinal neurodegeneration could be based on paracrine stem cell properties.^{1,3,4} Our results showed that retinal neurodegeneration did not modify the MSC phenotype;²⁷ therefore, during the 72 h of the experiment, the MSCVs could have been secreting paracrine factors that induce a neuroprotective effect over the photoreceptor cells. In this scenario, we performed the analysis of the bone marrow MSC protein profile on the basis that the secretome may be different depending on the extracellular environment. Therefore, we evaluated the protein profile secreted by MSCs in a “neurodegenerative condition” (neuroretinal explants cocultured with MSCs), and we also studied the secretome of MSC cultures alone, which allowed us to compare the protein profile secreted by the stem cells “per se” and under neuroretinal degeneration. The complete analysis of the secretome showed that 501 proteins display a higher expression levels in the MSCVs co-cultured with neuroretinas than in the mono-cultured MSCVs. These presented proteins are coming from two possible sources, i.e., secretion by the degenerating neuroretinas or by the MSCVs cultured with the neuroretinas. An inflammatory response, oxidative stress, and activation of apoptotic pathways are common features in the retinal neurodegenerative processes;¹ therefore, the origin of the proteins implicated in these pathways could be retinal neurodegeneration. However, the secreted proteins by MSCVs may be involved in retinal neuroprotection. Previously, it has been described that several proteins such as glial-derived neurotrophic factor (GDNF), brain-derived neurotrophic factor (BDNF), platelet-derived growth factor (PDGF), and ciliary neurotrophic factor (CNTF) were implicated in retinal neuroprotection by the paracrine effects of human bone marrow MSC,^{11,28} which are confirmed with the current results. Other proteins such as erythropoietin, Dll4, insulin growth factor (IGF), nerve growth factor (NGF), fibroblast growth factor (FGF), or pigment

Table 1. Primary Antibodies Used and Their Experimental Conditions

Molecular Marker	Origin	Source	Sample Processing	Dilution	Time (h)	Temp.
Human Bone Marrow Mesenchymal Stem Cells						
Cluster of differentiation present on B lymphocytes (CD19)	monoclonal mouse	Millipore, #SCR067	methanol fixed	1:500	12	4°C
Cluster of differentiation present on leukocytes (CD14)	monoclonal mouse	Millipore, #SCR067	methanol fixed	1:500	12	4°C
Homing cell adhesion molecule (H-CAM or CD44)	monoclonal mouse	Millipore, #SCR067	methanol fixed	1:500	12	4°C
Melanoma cell adhesion molecule (M-CAM or CD146)	monoclonal mouse	Millipore, #SCR067	methanol fixed	1:500	12	4°C
Stromal precursor antigen-1 (STRO-1)	monoclonal mouse	Millipore, #SCR067	methanol fixed	1:500	12	4°C
Thy-1 cell surface antigen (THY-1 or CD90)	monoclonal mouse	Millipore, #SCR067	methanol fixed	1:500	12	4°C
Neuroretinal Explants						
Glial fibrillary acidic protein (GFAP)	polyclonal rabbit	Dako, #n1506	paraffin	1:250	1	RT
Peanut agglutinin (PNA) lectin	arachis hypogaea	Molecular Probes, #L-21458	cryosectioned	1:100	1	RT
Protein kinase C α (PKC α) isoform	polyclonal rabbit	Santa Cruz Biotechnology, #SC-108000	paraffin	1:100	12	RT
Rhodopsin (Rho)	polyclonal rabbit	Chemicon-Millipore, #AB9279	paraffin	1:100	12	4°C

Temp., temperature; RT, room temperature.

epithelium-derived factor (PEDF) also have been associated with retinal neuroprotection;^{10,29–31} however, to the best of our knowledge, this is the first report of photoreceptor neuroprotection mediated by these paracrine factors of human bone marrow MSCs. Our results also showed higher expression levels of neuroprotective proteins such as Crim1, Glupican3, Cntn1, or Tmeff2; thus, this is the first time that they were associated with the retinal neuroprotection mediated by human bone marrow MSCs. Retinal degeneration leads to protein misfolding, so understanding the mechanisms that maintain and re-establish retinal protein homeostasis is crucial for developing new therapeutic approaches.¹⁸ The neuroretinal cells have evolved many mechanisms to cope with misfolded proteins, including the heat shock response, the unfolded protein response, and autophagy. These mechanisms, referred to as proteostasis (protein homeostasis), generate and maintain correctly folded proteins and remove misfolded proteins to maintain the normal cellular function.^{18,32} Our results showed higher levels of Hsp10, Hsp20, Hsp27, Hsp60, Hsp70, clusterin, Kctd10, and Pyk2 proteins in the neuroretinas co-cultured with MSCVs, which are implicated in proteostasis via heat shock protein and unfolded protein responses.^{33,34} Thus, the co-culturing of neuroretinas with MSCVs may activate the mechanisms of protein homeostasis to fight the neurodegenerative process. Finally, the results also showed the expression of proteins with antioxidant activity (haptoglobin³⁵), anti-apoptotic role (Apex1),³⁶ and with anti-inflammatory activity (transforming growth factor- β and interleukins 10, 11, 13, and 4),³⁷ which may slow retinal neurodegeneration. Several potential risks are associated with stem cell-based therapies, such as engraftment at an ectopic location, inappropriate differentiation, or aggregate formation.³⁸ Therefore, knowing the MSC secretome with retinal neuroprotective properties may be crucial for developing

cell-free compositions that allow use of a safe alternative to stem cell transplantation and avoid the potential risks. Besides, handling and storage of compositions based in the MSC secretome present important advantages over living cells in clinical practice.³⁹

In summary, this study showed that human bone marrow MSCs favor preservation of the neuroretinal general structure and organization, reduce reactive gliosis, and preserve retinal neurons, mainly photoreceptors, from degeneration via secretion of proteins involved in the neuroprotective processes. These results are in line with those reported previously by our group; we determined that MSCs can improve the survival and maintenance of RGCs through the paracrine neuroprotective potential of the MSCs.¹¹ The current results reinforced the hypothesis that the paracrine effect of the human bone marrow MSCs preserves the general retinal structure and organization by the secretion of proteins involved in neuroprotective processes. Therefore, *in vitro* evidence showed that a MSC secretome may be a therapeutic option in the treatment of retinal degenerative diseases.

MATERIALS AND METHODS

Cell Culture and Culture Conditions

Human bone marrow MSCs from different healthy adult donors were provided by Cytospin (MSCVs, Valladolid, Spain) after characterization, as reported previously.^{40–42} In brief, MSCVs are positive for the mesenchymal stem cell antigens (CD105, CD90, CD73, and CD166), established by the International Society for Cell Therapy (ISCT), and negative for specific markers of hematopoietic cells (CD14, CD34, CD45, and histocompatibility leukocyte antigen [HLA]-DR). MSCVs are produced under good manufacturing practice (GMP) regulations

Table 2. Relevant Proteins with Significantly Higher Expression in Human Bone Marrow MSCs Co-cultured with Neuroretinas Compared with Mono-Cultured Bone Marrow MSCs

Inflammation/Immunity							
IL-1F5	IL-1F7	IL-1F8	IL-1R4	IL-1ra	IL-2R α	IL-2R γ	IL-3
IL-3R α	IL-4R	IL-5	IL-6R	IL-7	IL-8	IL-10	IL-10R α
IL-10R β	IL-11	IL-12 p40	IL-12 p70	IL-12R β 2	IL-13	IL-15R α	IL-16
IL-17B	IL-17BR	IL-17C	IL-17D	IL-17E	IL-18 BPa	IL-18R α	IL-18R β
IL-19	IL-20	IL-20R α	IL-20R β	IL-21	IL-22	IL-22 BP	IL-23R
IL-24	IL-26	IL-27	IL-29	IL-31	haptoglobin	CXCR6	TNFRSF17
CD14	CD30L	CD40L	IL-8RB	CXCR3	CXCR4 (fusin)	DcR3	HCR
CD46	CD55	CD61	CD71	CD74	CD79 α	CD90	CD97
CD200	IGF-II	ICAM-2	ICAM-3	ICAM-5	IFN- α	IFN- β	GLO-1
HVEM	I-TAC	LECT2	MCP-1	MCP-2	MCP-3	L-selectin	TNFRSF3
MIP-1b	MIP 2	MIP-3 β	MICA	RANTES	OX40L	PARC	pentraxin 3
PF4	P-selectin	TNFRSF19L	TNFRSF13B	thymopietin	TLR2	TLR3	TLR4
TRAIL	TRAIL R1	TRAILR4	ADAMTS-1	ADAMTS-19	ADAMTS-4	AMICA	BLAME
CFHR2	CHI3L1	chymase	DPPIV	FAP	Fc RIIB/C	fibrinopeptide A	ficolin 3
FOXP3	furin	GATA-3	IL-33	IL-34	IL36RN	Itk	LAG-3
legumain	LOX-1	LTF	MATK	MBL	MICB	midkine	Notch-1
OX40	pappalysin-1	PD-1	PYK2	Tec	TIM-1	adiponectin	hepassocin
TIMP-1	ALCAM	EpCAM	OSM	IGF-1	Csk	Smad4	Ck β 8-1
ghrelin	COX2	leptin R	THFSF3	TCCR/WSX-1	C3a		
Death and Cell Survival							
Pro-apoptosis		Cell Survival		Pro-apoptosis/Cell Survival			Autophagy
PPP2R5C	RIP1	HSP10	clusterin	CCR4	CD27/TNFRSF7		FOXO1
FAM3B	SMAC	HSP20	MINA	HGF	mer		PI3K p85 β
BAX	TOPORS	HSP27	NAIP	NOV/CCN3	Livin		
BIK	TGF- β 1	HSP60	NELL2	SCFR/CD117	IFN- α		
caspase-3	TGF- β 5	HSP70	PAK7	WISP-1/CCN4	IFN- β		
caspase-8	FAK	HSP90	PIM2	BNIP2	LRP-1		
IGFBP-3	FRK	HSPA8	PTN	survivin	lipocalin-2		
protein p65	galectin-1	ROS					
Cellular/Oxidative Stress				Retinol Metabolism			
haptoglobin	APEX-1	VDUP-1			RBP4		
Collagen Metabolism							
MMP-8	MMP-11	NCAM-1	MMP-1	MMP-2	MMP-7	MMP-9	MMP-10
MMP-12	MMP-13	MMP-14	MMP-15	MMP-16	MMP-19	pro-MMP-7	pro-MMP-9
pro-MMP-13							
Lipid Metabolism							
ApoA1	ApoA2	SERTAD2	BMPR-II	BMPR-IA	ApoA4	ApoC2	ApoD
ApoE	ApoE3	FABP1	FABP4	resistin	vitronectin	LRP-1	
Angiogenesis							
angiotatin	endothelin	VEGFR2	angiopoietin-2	angiopoietin-4	angiopoietin-like 2	NF1	angiopoietin-like 1
FGFR2							
Neuroprotection							
DLL4	nestin	NPTX1	NPTXR	PEDF	BDNF	AR (amphiregulin)	CRIM1

(Continued on next page)

Table 2. Continued

Inflammation/Immunity							
GFR α -4	glypican 3	glypican 5	NGF	NrCAM	neuritin	thrombospondin 4	TMEFF2
CNTN1	IGF2BP1	ITM2B	Pro-BDNF	RECK	ROR1	TPA	chordin-like1
PDGF-AA	PDGF-C	PDGF-D	erythropoietin	NT-3	FGF		
Calcium Metabolism							
ApoA1	SERTAD2	ALK-3	ApoC1	ApoD	ApoE3	FABP4	vitronectin
ApoA2	BMPR-II	ApoA4	ApoC2	ApoE	FABP1	resistin	

and have been approved by the Spanish Drug Agency (AEMPS) for several clinical trials of ophthalmology (European Union Drug Regulating Authorities Clinical Trials Database [EudraCT]: 2011-005321-51 and 2016-003029-40). Fresh MSCVs were provided in a vial containing 1×10^6 cells/mL. HEK293T cells, generously donated by Prof. González-Sarmiento from the University of Salamanca (Spain), were used as negative control of neuroprotection.²⁸ A trypan blue assay (Sigma-Aldrich, St. Louis, MO, USA) was used to determine cell viability and cell counts (TC20 automated cell counter; Bio-Rad, Hercules, CA, USA). The cells were seeded on the bottom of Transwell 24-mm-diameter culture plates (Corning Life Sciences, Corning, NY) in Dulbecco's modified Eagle's medium (DMEM) supplemented with 10% fetal bovine serum (Gibco, Invitrogen, Paisley, UK), 1% antibiotics (100 U/mL penicillin and 100 μ g/mL streptomycin) (Gibco, Invitrogen), and 1% L-glutamine (Sigma-Aldrich, St. Louis, MO, USA). We seeded 30,000 cells/well of MSCs, as previously reported by our group,^{11,21} and 10,000 cells/well of HEK293T cells. The cells were cultured at 37°C in a 5% CO₂ atmosphere for 72 h until confluence, for subsequent co-culturing with neuroretinal explants.

Central Neuroretinal Explant Preparation and Culture

Nine fresh porcine eyes from animals aged 6–8 months were obtained from a local slaughterhouse. Neuroretinal explants (n = 32) were obtained less than 2 h after enucleation, as previously described.^{11,21} Briefly, the eyes were dissected and the porcine area centralis (cone-enriched visual streak without blood vessels) was identified. Four adjacent explants from the area centralis were obtained from each eye. The neuroretinal explants were laid over Transwell membranes 24 mm in diameter with a 0.4- μ m pore polycarbonate membrane insert (Corning Life Sciences) with the photoreceptor layer facing the membrane. The explants were cultured alone or with MSCVs or with HEK293T cells in the same culture well but physically separated by the Transwell porous membrane, which prevented cellular migration and integration into the neuroretinal tissue. The co-cultures were maintained in DMEM/Neurobasal A medium (1:1) (Gibco) supplemented with 10% fetal bovine serum, 1% antibiotics, 2% B-27, and 1% L-glutamine under standard culture conditions for 72 h. Contact between the culture medium (1.5 mL, as suggested by the manufacturer) and the support membrane beneath the explants was maintained by changing the culture medium with freshly prepared medium. The medium was entirely changed daily and stored at –80°C for secretome analysis. Furthermore, neuroretinal explants were obtained and processed in parallel before culturing (fresh neuroretinas).

Five experimental conditions were evaluated for a total of 45 experiments as follows: mono-cultured MSCVs (n = 9), mono-cultured neuroretinal explants (n = 9), neuroretinal explants co-cultured with MSCVs (n = 9), neuroretinal explants co-cultured with HEK293T cells (n = 9), and fresh neuroretinas (n = 9).

Neuroretinal Histologic and Immunochemical Characterization

Fresh or cultured neuroretinal explants were fixed with 4% paraformaldehyde (Panreac Quimica, Barcelona, Spain) in phosphate-buffered saline (PBS) for 2 h at 4°C, and each explant was cut in half. Half of the samples were embedded in paraffin (Paraplast Plus, Leica Biosystems, Nussloch, Germany) using an automatic tissue processor (ASP300, Leica Microsystems, Wetzlar, Germany), and 4- μ m sections were obtained with a rotatory microtome (RM2145, Leica Microsystems). The other halves of the samples were subjected to sucrose (Panreac Quimica cryoprotection, embedded in Tissue-Tek OCT compound (Sakura Finetek Europe, Alphen, the Netherlands), and cut into 12- μ m sections on a cryostat (CM1900, Leica Microsystems).

Paraffin-embedded sections were deparaffinized in xylene (Sigma-Aldrich) and rehydrated in decreasing ethanol concentrations. The sections then were stained with hematoxylin and eosin (Sigma-Aldrich) or processed for immunochemistry by incubating with 0.01% trypsin for 1 h and blocking in PBS with 5% goat serum for 2 h at room temperature. Frozen neuroretinal sections processed for immunochemistry were thawed, washed in water, and blocked in PBS with 5% goat serum and 0.1% Triton X-100 (Sigma-Aldrich) for 2 h at room temperature. The primary antibodies used and their conditions are summarized in Table 1. The corresponding species-specific secondary antibodies conjugated to Alexa Fluor 568 (red) (1:200, Molecular Probes) were then applied. The nuclei were stained with 4',6-diamidino-2-phenylindole (DAPI) (10 μ g/mL, Molecular Probes). Finally, the samples were mounted in fluorescent mounting medium (Dako, Glostrup, Denmark) and coverslipped. Fluorescence images were captured with a Leica TCS SP5 DMI-6000B confocal microscope (Leica Microsystems) and analyzed with Leica LAS AF software. The final processing and composition of the figures were performed with Pixelmator 3.8.2 Phoenix (Pixelmator Team, Vilnius, Lithuania).

Semiquantitative immunohistochemical analysis was performed using ImageJ software (version 1.49, National Institutes of Health, Bethesda, MD, USA) on $\times 20$ fluorescence images from non-serial neuroretinal sections (n = 5 sections per sample). Comparative analyses

of images acquired at the same levels of exposure, intensity, and gain were performed. Two-channel micrographs were analyzed as previously described,⁴³ and the micrographs were then split into different channels and each channel thresholded. The background in the red channel (corresponding to the protein of interest) was subtracted by using a threshold value obtained from negative controls. The same value was used for all images from a single experiment analyzed in a single session. The threshold for the blue channel, corresponding to the area of nuclei, was set according to the area stained. Mean gray value was measured by redirecting the measurement to the corresponding channel. The results, in arbitrary units (a.u.), were the ratio of the mean gray value for the red channel.

Neuroretinal Morphometry and Cell Counts

Neuroretinal parenchyma was analyzed by measuring the total thickness between the outer limiting membrane and the inner limiting membrane. The thicknesses of the ONL, OPL, INL, IPL, and GCL, including the NFL, were also measured. Measurements were performed using ImageJ software (version 1.49, National Institutes of Health, Bethesda, MD, USA) on $\times 20$ images from non-serial hematoxylin-stained neuroretinal sections ($n = 5$ sections/sample). DAPI-stained nuclei were quantified automatically by the ImageJ software and the plugin RetFM-J.IS.⁴⁴ A masked researcher performed all neuroretinal thickness measurements and nucleus quantifications in triplicate.

MSC Immunochemical Characterization

The MSCVs were fixed on the bottom of the Transwell culture plates with ice-cold methanol (Panreac Quimica) for 15 min at 4°C and then immunostained with a human MSC characterization kit (Millipore, Billerica, MA, USA). Primary antibodies (Table 1) were applied overnight in a ratio of 1:500 at 4°C. The corresponding species-specific secondary antibody conjugated to Alexa Fluor 488 (green, 1:200; Molecular Probes, Eugene, OR, USA) was applied for 2 h at room temperature. The nuclei were stained with DAPI (10 $\mu\text{g}/\text{mL}$). Finally, samples were mounted in fluorescent mounting medium (Dako, Demark) and coverslipped. Fluorescence images were captured with a Leica TCS SP5 DMI-6000B confocal microscope and were analyzed with Leica LAS AF software. The final processing and composition of the figures were performed with Pixelmator 3.8.2 Phoenix.

Protein Microarray Assay

For the protein profile analysis, collected culture media from stem cells cultured alone and from stem cells co-cultured with neuroretina were pooled to study the overall protein content over the entire experimental period. A human antibody array (RayBiotech, Peachtree Corners, GA, USA) was used according to the manufacturer's guidelines to simultaneously detect the relative expression of 1,000 human proteins in cell culture supernatants. The protein concentration of each supernatant was determined in the range of 7–8 $\mu\text{g}/\text{mL}$ using a BCA (bicinchoninic acid) protein assay (Pierce BCA protein assay kit, catalog no. 23227, Sigma-Aldrich, St. Louis, MO, USA). All samples were dialyzed against $1 \times$ PBS (pH 8.0) (as a dialysis buffer). Ten micrograms of each sample was then biotinylated according to the

manufacturer's instructions. The biotinylation was evaluated in all samples using a Pierce biotin quantitation kit to ensure equal conditions for all samples. The antibody arrays were blocked at 4°C with RayBiotech blocking buffer $1 \times$. All biotinylated samples were incubated in the same comparable conditions as previously described by Díez et al.⁴⁵ After incubation, all of the arrays were incubated with RayBiotech horseradish peroxidase (HRP)-streptavidin $1 \times$. The array images were acquired using a ChemiDoc MD (Bio-Rad, CA, USA) as a conventional western blot procedure at the optimized exposition. Semiquantitative data analysis was performed according to the RayBio analysis tool guidelines.^{46–48} All experimental conditions were performed in triplicate.

Data Acquisition and Statistical Analysis

All data were collected in an Excel database (Microsoft Office Excel, 2016, Microsoft, Redmond, WA, USA). SPSS (version 24.0, SPSS, Chicago, IL, USA) was used for statistical analyses. After confirming the data homogeneity of variance and normal distribution, we performed analysis of variance followed by pairwise comparisons (Bonferroni test). For non-parametric variables, the group means were compared using the Mann-Whitney U test (two groups) or the Kruskal-Wallis test (more than two groups). Differences were considered significant at $p < 0.05$.

SUPPLEMENTAL INFORMATION

Supplemental Information can be found online at <https://doi.org/10.1016/j.omtm.2020.05.003>.

AUTHOR CONTRIBUTIONS

Conception and Design: R.U.M., J.C.P., and I.F.-B.; Experimental Work: R.U.M., K.P.-N., M.-T.G.-G., and M.F.; Analysis and Interpretation of Data: R.U.M., K.P.-N., and I.F.-B.; Drafting the Article: R.U.M. and I.F.-B.; Revising the Article: all authors; Study Supervision: I.F.-B.

CONFLICTS OF INTEREST

The authors declare no competing interests.

ACKNOWLEDGMENTS

The authors are grateful to the staff of the Justino Gutierrez S.L. Slaughterhouse (Valladolid, Spain) for providing the porcine eye globes used in this work and to Citospin S.L. (Valladolid, Spain) for providing the MSCs used in this work. We also thank Lynda Charters from Medical International (Framingham, MA, USA) for his assistance in the final editing and preparation of this manuscript. This work was supported by grants from Fondo Europeo de Desarrollo Regional (FEDER) and Consejería de Educación from Junta de Castilla y León, Spain (grant VA077P17), and from the Spanish Health Institute Carlos III (ISCIII) (grants PI17/01930 and CB16/12/00400). The Proteomics Unit belongs to ProteoRed (PRB3-ISCIII) supported by grant PT17/0019/0023, of the PEI+D+I 2017-2020, funded by ISCIII and FEDER. R.U.-M. was supported by FEDER and Consejería de Educación from Junta de Castilla y León, Spain (grant VA077P17); K.P.-N. was supported by Fundación Carolina,

Madrid, Spain; and I.F.-B. was supported by Centro en Red de Medicina Regenerativa y Terapia Celular, Junta de Castilla y León, Spain.

REFERENCES

- Cuenca, N., Fernández-Sánchez, L., Campello, L., Maneu, V., De la Villa, P., Lax, P., and Pinilla, I. (2014). Cellular responses following retinal injuries and therapeutic approaches for neurodegenerative diseases. *Prog. Retin. Eye Res.* *43*, 17–75.
- Gagliardi, G., Ben M'Barek, K., and Goureau, O. (2019). Photoreceptor cell replacement in macular degeneration and retinitis pigmentosa: a pluripotent stem cell-based approach. *Prog. Retin. Eye Res.* *71*, 1–25.
- Tang, Z., Zhang, Y., Wang, Y., Zhang, D., Shen, B., Luo, M., and Gu, P. (2017). Progress of stem/progenitor cell-based therapy for retinal degeneration. *J. Transl. Med.* *15*, 99.
- Bhattacharya, S., Gangaraju, R., and Chaum, E. (2017). Recent advances in retinal stem cell therapy. *Curr. Mol. Biol. Rep.* *3*, 172–182.
- MacLaren, R.E., Pearson, R.A., MacNeil, A., Douglas, R.H., Salt, T.E., Akimoto, M., Swaroop, A., Sowden, J.C., and Ali, R.R. (2006). Retinal repair by transplantation of photoreceptor precursors. *Nature* *444*, 203–207.
- Mellough, C.B., Cui, Q., and Harvey, A.R. (2007). Treatment of adult neural progenitor cells prior to transplantation affects graft survival and integration in a neonatal and adult rat model of selective retinal ganglion cell depletion. *Restor. Neurol. Neurosci.* *25*, 177–190.
- Waldron, P.V., Di Marco, F., Kruczek, K., Ribeiro, J., Graca, A.B., Hippert, C., Aghaizu, N.D., Kalargyrou, A.A., Barber, A.C., Grimaldi, G., et al. (2018). Transplanted donor- or stem cell-derived cone photoreceptors can both integrate and undergo material transfer in an environment-dependent manner. *Stem Cell Reports* *10*, 406–421.
- Johnson, T.V., Bull, N.D., and Martin, K.R. (2009). Transplantation prospects for the inner retina. *Eye (Lond.)* *23*, 1980–1984.
- Hill, A.J., Zwart, I., Tam, H.H., Chan, J., Navarrete, C., Jen, L.S., and Navarrete, R. (2009). Human umbilical cord blood-derived mesenchymal stem cells do not differentiate into neural cell types or integrate into the retina after intravitreal grafting in neonatal rats. *Stem Cells Dev.* *18*, 399–409.
- Kolomeyer, A.M., and Zarbin, M.A. (2014). Trophic factors in the pathogenesis and therapy for retinal degenerative diseases. *Surv. Ophthalmol.* *59*, 134–165.
- Labrador-Velandia, S., Alonso-Alonso, M.L., Di Lauro, S., García-Gutiérrez, M.T., Srivastava, G.K., Pastor, J.C., and Fernandez-Bueno, I. (2019). Mesenchymal stem cells provide paracrine neuroprotective resources that delay degeneration of co-cultured organotypic neuroretinal cultures. *Exp. Eye Res.* *185*, 107671.
- Xu, W., and Xu, G.-X. (2011). Mesenchymal stem cells for retinal diseases. *Int. J. Ophthalmol.* *4*, 413–421.
- Salehi, H., Amirpour, N., Razavi, S., Esfandiari, E., and Zavar, R. (2017). Overview of retinal differentiation potential of mesenchymal stem cells: a promising approach for retinal cell therapy. *Ann. Anat.* *210*, 52–63.
- Nauta, A.J., and Fibbe, W.E. (2007). Immunomodulatory properties of mesenchymal stromal cells. *Blood* *110*, 3499–3506.
- Ankrum, J.A., Ong, J.F., and Karp, J.M. (2014). Mesenchymal stem cells: immune evasive, not immune privileged. *Nat. Biotechnol.* *32*, 252–260.
- Berglund, A.K., Fortier, L.A., Antczak, D.F., and Schnabel, L.V. (2017). Immunoprivileged no more: measuring the immunogenicity of allogeneic adult mesenchymal stem cells. *Stem Cell Res. Ther.* *8*, 288.
- Labrador Velandia, S., Di Lauro, S., Alonso-Alonso, M.L., Tabera Bartolomé, S., Srivastava, G.K., Pastor, J.C., and Fernandez-Bueno, I. (2018). Biocompatibility of intravitreal injection of human mesenchymal stem cells in immunocompetent rabbits. *Graefes Arch. Clin. Exp. Ophthalmol.* *256*, 125–134.
- Athanasiou, D., Aguilà, M., Bevilacqua, D., Novoselov, S.S., Parfitt, D.A., and Cheetham, M.E. (2013). The cell stress machinery and retinal degeneration. *FEBS Lett.* *587*, 2008–2017.
- Ruether, K., Feigenspan, A., Pirngruber, J., Leitges, M., Baehr, W., and Strauss, O. (2010). PKC α is essential for the proper activation and termination of rod bipolar cell response. *Invest. Ophthalmol. Vis. Sci.* *51*, 6051–6058.
- Vecino, E., Rodriguez, F.D., Ruzafa, N., Pereiro, X., and Sharma, S.C. (2016). Glia-neuron interactions in the mammalian retina. *Prog. Retin. Eye Res.* *51*, 1–40.
- Di Lauro, S., Rodríguez-Crespo, D., Gayoso, M.J., García-Gutiérrez, M.T., Pastor, J.C., Srivastava, G.K., and Fernandez-Bueno, I. (2016). A novel coculture model of porcine central neuroretina explants and retinal pigment epithelium cells. *Mol. Vis.* *22*, 243–253.
- Garlipp, M.A., Nowak, K.R., and Gonzalez-Fernandez, F. (2012). Cone outer segment extracellular matrix as binding domain for interphotoreceptor retinoid-binding protein. *J. Comp. Neurol.* *520*, 756–769.
- Fernandez-Bueno, I., Fernández-Sánchez, L., Gayoso, M.J., García-Gutiérrez, M.T., Pastor, J.C., and Cuenca, N. (2012). Time course modifications in organotypic culture of human neuroretina. *Exp. Eye Res.* *104*, 26–38.
- Bringmann, A., and Wiedemann, P. (2012). Müller glial cells in retinal disease. *Ophthalmologica* *227*, 1–19.
- Mollick, T., Mohlin, C., and Johansson, K. (2016). Human neural progenitor cells decrease photoreceptor degeneration, normalize opsin distribution and support synapse structure in cultured porcine retina. *Brain Res.* *1646*, 522–534.
- Jones, M.K., Lu, B., Chen, D.Z., Spivia, W.R., Mercado, A.T., Ljubimov, A.V., Svendsen, C.N., Van Eyk, J.E., and Wang, S. (2019). In vitro and in vivo proteomic comparison of human neural progenitor cell-induced photoreceptor survival. *Proteomics* *19*, e1800213.
- Delorme, B., Ringe, J., Gallay, N., Le Vern, Y., Kerboeuf, D., Jorgensen, C., Rosset, P., Sensebé, L., Layrolle, P., Häupl, T., and Charbord, P. (2008). Specific plasma membrane protein phenotype of culture-amplified and native human bone marrow mesenchymal stem cells. *Blood* *111*, 2631–2635.
- Johnson, T.V., DeKorver, N.W., Levasseur, V.A., Osborne, A., Tassoni, A., Lorber, B., Heller, J.P., Villasmil, R., Bull, N.D., Martin, K.R., and Tomarev, S.I. (2014). Identification of retinal ganglion cell neuroprotection conferred by platelet-derived growth factor through analysis of the mesenchymal stem cell secretome. *Brain* *137*, 503–519.
- Luo, H., Jin, K., Xie, Z., Qiu, F., Li, S., Zou, M., Cai, L., Hozumi, K., Shima, D.T., and Xiang, M. (2012). Forkhead box N4 (Foxn4) activates Dll4-Notch signaling to suppress photoreceptor cell fates of early retinal progenitors. *Proc. Natl. Acad. Sci. USA* *109*, E553–E562.
- Ding, S.L.S., Koh, A.E., Kumar, S., Ali Khan, M.S., Alzahrani, B., and Mok, P.L. (2019). Genetically-modified human mesenchymal stem cells to express erythropoietin enhances differentiation into retinal photoreceptors: an in-vitro study. *J. Photochem. Photobiol. B* *195*, 33–38.
- Vigneswara, V., and Ahmed, Z. (2019). Pigment epithelium-derived factor mediates retinal ganglion cell neuroprotection by suppression of caspase-2. *Cell Death Dis.* *10*, 102.
- Balch, W.E., Morimoto, R.I., Dillin, A., and Kelly, J.W. (2008). Adapting proteostasis for disease intervention. *Science* *319*, 916–919.
- Vembar, S.S., and Brodsky, J.L. (2008). One step at a time: endoplasmic reticulum-associated degradation. *Nat. Rev. Mol. Cell Biol.* *9*, 944–957.
- Vabulas, R.M., Raychaudhuri, S., Hayer-Hartl, M., and Hartl, F.U. (2010). Protein folding in the cytoplasm and the heat shock response. *Cold Spring Harb. Perspect. Biol.* *2*, a004390.
- Tseng, C.F., Lin, C.C., Huang, H.Y., Liu, H.C., and Mao, S.J.T. (2004). Antioxidant role of human haptoglobin. *Proteomics* *4*, 2221–2228.
- Dyballa-Rukes, N., Jakobs, P., Eckers, A., Ale-Agha, N., Serbulea, V., Aufenvenne, K., Zschauer, T.C., Rabanter, L.L., Jakob, S., von Arnell, F., et al. (2017). The anti-apoptotic properties of APEX1 in the endothelium require the first 20 amino acids and converge on thioredoxin-1. *Antioxid. Redox Signal.* *26*, 616–629.
- Turner, M.D., Nedjai, B., Hurst, T., and Pennington, D.J. (2014). Cytokines and chemokines: at the crossroads of cell signalling and inflammatory disease. *Biochim. Biophys. Acta* *1843*, 2563–2582.
- Herberts, C.A., Kwa, M.S.G., and Hermsen, H.P.H. (2011). Risk factors in the development of stem cell therapy. *J. Transl. Med.* *9*, 29.
- Vizoso, F.J., Eiro, N., Cid, S., Schneider, J., and Perez-Fernandez, R. (2017). Mesenchymal stem cell secretome: toward cell-free therapeutic strategies in regenerative medicine. *Int. J. Mol. Sci.* *18*, E1852.

40. Orozco, L., Soler, R., Morera, C., Alberca, M., Sánchez, A., and García-Sancho, J. (2011). Intervertebral disc repair by autologous mesenchymal bone marrow cells: a pilot study. *Transplantation* 92, 822–828.
41. Orozco, L., Munar, A., Soler, R., Alberca, M., Soler, F., Huguet, M., Sentís, J., Sánchez, A., and García-Sancho, J. (2013). Treatment of knee osteoarthritis with autologous mesenchymal stem cells: a pilot study. *Transplantation* 95, 1535–1541.
42. Vega, A., Martín-Ferrero, M.A., Del Canto, F., Alberca, M., García, V., Munar, A., Orozco, L., Soler, R., Fuertes, J.J., Huguet, M., et al. (2015). Treatment of knee osteoarthritis with allogeneic bone marrow mesenchymal stem cells: a randomized controlled trial. *Transplantation* 99, 1681–1690.
43. Soriano-Román, L., Contreras-Ruiz, L., García-Posadas, L., López-García, A., Masli, S., and Diebold, Y. (2015). Inflammatory cytokine-mediated regulation of thrombospondin-1 and CD36 in conjunctival cells. *J. Ocul. Pharmacol. Ther.* 31, 419–428.
44. Hedberg-Buenz, A., Christopher, M.A., Lewis, C.J., Meyer, K.J., Rudd, D.S., Dutca, L.M., Wang, K., Garvin, M.K., Scheetz, T.E., Abramoff, M.D., et al. (2016). RetFM-J, an ImageJ-based module for automated counting and quantifying features of nuclei in retinal whole-mounts. *Exp. Eye Res.* 146, 386–392.
45. Díez, P., Lorenzo, S., Dégano, R.M., Ibarrola, N., González-González, M., Nieto, W., Almeida, J., González, M., Orfao, A., and Fuentes, M. (2016). Multipronged functional proteomics approaches for global identification of altered cell signalling pathways in B-cell chronic lymphocytic leukaemia. *Proteomics* 16, 1193–1203.
46. Díez, P., Dasilva, N., González-González, M., Matarraz, S., Casado-Vela, J., Orfao, A., and Fuentes, M. (2012). Data analysis strategies for protein microarrays. *Microarrays (Basel)* 1, 64–83.
47. González-González, M., Bartolome, R., Jara-Acevedo, R., Casado-Vela, J., Dasilva, N., Matarraz, S., García, J., Alcazar, J.A., Sayagues, J.M., Orfao, A., and Fuentes, M. (2014). Evaluation of homo- and hetero-functionally activated glass surfaces for optimized antibody arrays. *Anal. Biochem.* 450, 37–45.
48. León, I.E., Díez, P., Etcheverry, S.B., and Fuentes, M. (2016). Deciphering the effect of an oxovanadium(IV) complex with the flavonoid chrysin (VOChrysin) on intracellular cell signalling pathways in an osteosarcoma cell line. *Metallomics* 8, 739–749.